Rare Metal Materials and Engineering
Volume 50, Issue 2, February 2021
Available online at www.rmme.ac.cn

Science Press

Cite this article as: Rare Metal Materials and Engineering, 2021, 50(2): 0408-0415.

ARTICLE

Effect of Process Parameter Settings and Thickness on Microstructures of EBM Produced Ti-6Al-4V Alloy

He Huaizhi[1,2,3], Safdar Adnan[1], Wei Liuying[1]

[1] Division of Materials Science, Malmö University, Malmö SE-205 06, Sweden; [2] State Key Laboratory of Advanced Welding and Joining, Harbin Institute of Technology, Harbin 150001, China; [3] Central Academy, Harbin Electric Corporation, Harbin 150028, China

Abstract: The effect of sample dimensions and process parameters (beam current, scan speed, offset focus and scan length) of electron beam melting (EBM) system on microstructure of the EBM built Ti-6Al-4V alloy was investigated. The microstructure of EBM built Ti-6Al-4V alloy consists of columnar grains of prior β phase. Inside the columnar grain, typical (α+β) structures, namely Widmanstätten α platelets and rod-like β phase formed on the interfaces of the fine α grains, are observed. Grain boundary α layer forms along grain boundary of prior β columnar grain. With the increase of thickness of the test slab, beam energy density and scanning length, the prior β columnar grain grows along the build direction and diameter of which increases. The columnar grain diameter also decreases with the increase in height of the test slab. With increasing the thickness of the test slab and beam energy density, α platelets get coarser.

Key words: Ti-6Al-4V; EBM; process parameters

Over the past two to three decades, many additive manufacturing (AM) techniques have been investigated to fabricate fully dense and near net shape metal parts for variety of applications. The basic concept behind all AM techniques is to take mass produced raw material with innovative processing technique for generating a finished component with minimum use of specialized or dedicated tools. In comparison to conventional methods, all AM methods have the advantage of reducing material waste, shorter lead time, minimum or zero tooling cost and high component complexity[1]. AM process is also widely used for building complex geometries like downward facing surfaces and complex functional parts as a single unit, avoiding machining, welding, etc[2,3].

Electron beam melting (EBM) is one of the AM methods. EBM process is energy efficient and can possess high coupling efficiency with deposited materials. Thus it is applicable to highly reflective materials such as aluminum[2,4]. EBM systems involve building of three-dimensional fully dense or near net-shape metallic structures/objects using high energy focused electron beam in high vacuum environment[2,3,5-8]. In EBM systems, each part builds in two steps. Firstly, the outer part/boundary melts, namely "contour". The contour provides an interface between the actual build and the surrounding powder. Contour melting also provides an opportunity to have good surface structure. In the second step of melting, the actual part builds within the contours. This part is normally referred as "squares".

Owing to the excellent combination of mechanical and physical properties, titanium and its alloys, especially Ti-6Al-4V alloy, are widely used as engineering materials in aerospace, automotive, energy and medical implant industries. The mechanical properties of Ti-6Al-4V show strong dependence on the metallurgical microstructures. The control of texture and microstructure is necessary to control the physical and mechanical properties of Ti-6Al-4V alloy[9,10]. The microstructures of Ti-6Al-4V alloy depend on the processing history and heat treatment[11]. This provides an opportunity to fabricate objects/parts with desired microstructures and mechanical properties by a set of optimized fabrication processes.

EBM process is a complex procedure depending upon

Received date: February 17, 2020
Foundation item: Knowledge Foundation Sweden (KKS0256)
Corresponding author: He Huaizhi, Master, Central Academy, Harbin Electric Corporation, Harbin 150028, P. R. China, Tel: 0086-451-58590367, E-mail: hehz@harbin-electric.com

different processing parameters of the system, including the beam power and size, scan speed and scanning direction/ scanning strategy. The final microstructures of EBMed Ti-6Al-4V alloy or any material are the result of complex combination under different processing parameters of the system. There is a possibility to obtain different microstructures of EBMed Ti-6Al-4V parts built with different sets of processing parameters. The object of this study is to investigate and understand the effect of mentioned different process parameters of EBM system such as beam current, beam offset focus, and scan speed on microstructures of EBM fabricated Ti-6Al-4V alloy test slabs by optical microscope (OM) and scanning electron microscope (SEM).

1 Experiment

In this study, four sets of rectangular test slabs (each set with contour and square, as shown in Fig.1) were produced by melting Ti-6Al-4V powder using Arcam's S12 EBM system under different process parameter settings. Each set consists of three slabs of approximately 55 mm×50 mm in two directions (x, y). Each test slab in the set has different thicknesses (w).

The contours are thin slabs with various thicknesses ranging from 1 mm to 2 mm. Squares are relatively thick slabs, in which both contours and squares are fully melted. The square slab melts with relatively high scan speed and beam current, and its thickness varies from 3.5 mm to 7.5 mm. Process parameter settings alter among the four sets according to the description in Table 1. To study the effect of scanning length, samples of 10 mm×10 mm in dimension and approximately 30 mm in height were prepared from another build.

To study the influence of different processing parameters, samples were obtained from the slabs produced under different parameter settings. To reduce the influence of other parameters on experimental results, samples having similar build up environment except the parameter of interest were chosen. The details of selected samples are listed in Table 2. Planes parallel to build direction were of major interest and accordingly the thin plane of varying thicknesses is marked as surface-I (S-I) and plane with 55 mm in width is marked as surface-II (S-II). The planes of a test slab are schematically illustrated in Fig.2.

Samples selected from different parts of the slabs for microstructure studies were prepared using standard metallographic procedures under similar conditions. Samples for optical and electron microscopic studies were first cut into slices of 2 mm in thickness and about 1 cm^2 in area. These slices were then grinded mechanically under flowing water

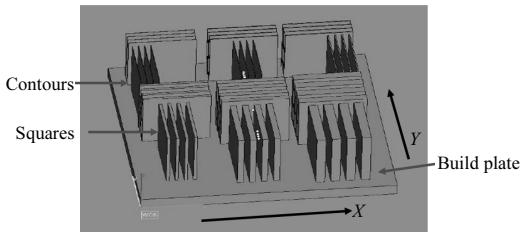

Fig.1 Schematic diagram of sample

Table 1 Parameter settings of different slabs

Test Slab		Sample code	Scan speed/ mm·s^{-1}	Current/ mA	Offset focus/ mA
Contour 1		C1	250	4	10
Contour 2		C2	250	6	10
Contour 3		C3	250	4	25
Contour 4		C4	250	6	25
Square 1	Contour	S1	180	8	15
	Square		575	9	15
Square 2	Contour	S2	180	8	15
	Square		650	9	15
Square 3	Contour	S3	180	8	30
	Square		575	9	30
Square 4	Contour	S4	180	8	30
	Square		650	9	30

Table 2 Selection of samples for comparative studies

Sample code	Width/mm	Scan speed/mm·s^{-1}		Focus/mA	Current/mA		Placement on plate
		Contour	Square		Contour	Square	
C1X2	2.09	250	-	10	4	-	*X*
C2X1	2.10	250	-	10	6	-	*X*
S1Y1	3.46	180	575	15	8	9	*Y*
S1Y2	5.50	180	575	15	8	9	*Y*
S1Y3	7.41	180	575	15	8	9	*Y*
S1X1	3.50	180	575	15	8	9	*X*
S1X2	5.50	180	575	15	8	9	*X*
S1X3	7.42	180	575	15	8	9	*X*
S3X3	7.42	180	575	30	8	9	*X*
S1X3	7.42	180	575	15	8	9	*X*
S2X3	7.40	180	650	15	8	9	*X*
S1X3	7.42	180	575	15	8	9	*X*

Notes: X and Y in sample code represent scanning direction is *X* and *Y*, respectively, as shown in Fig.1

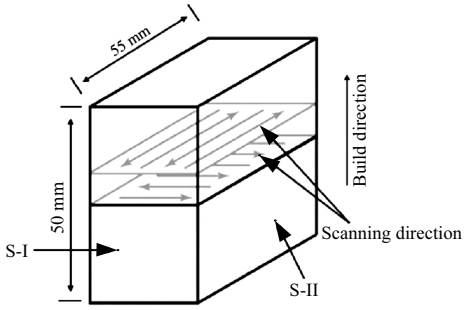

Fig.2 Schematic diagram of test slab and placement of samples

using silicon carbide papers from 220# to 800# to get thickness of ~1.5 mm. These samples were then electrochemically polished for 4~5 min by Struers double jet unit using electrolyte A3 (600 mL methanol, 360 mL 2-butoxyethanol and 60 mL perchloric acid). The electrochemical polishing voltage and average current were 35 V and ~400 mA, respectively. Samples mounted on plastic epoxy were gradually grinded by silicon carbide papers from 220# to 800# in the same way as the small samples, but in the final step, they were grinded with 9 μm diamond particle suspension to obtain smooth surface. In the next step, the samples were mechanically polished with OP suspension containing Al_2O_3 particles of 0.04 μm in H_2O_2 with pH=9.8 for different duration depending upon surface conditions. The average time of OP polishing was 4~5 min. In the final step, all samples were chemically etched for different duration of 2~7 min by Kroll's solution (1vol% HF+2vol% HNO_3+distilled H_2O).

Microstructures of different test slabs were studied by Nikon Elipse L150 optical microscope and EVOLS10 environmental scanning electron microscope (ESEM) with accelerating voltage of 20 kV.

2 Results

2.1 Build defects

The EBM system due to its nature and mode of operations is susceptible to introducing many defects in the EBM built materials. The sources of these defects can be attributed to the poor beam control, resulting in poor melting and undesired porosity. As the energy density of the beam depends upon different process parameters like beam current, offset focus and scan speed, the variation of these parameters has the potential to vastly influence the build quality.

In this study, most samples are defect-free irrespective of parameter settings. The only significant defects are observed in square samples S3 and S4, when the offset focus changes from 15 mA to 30 mA. The sample badly melts with higher offset focus, and undesired porosity of ~11% is observed (Fig.3a). Similar build defects were also reported by Gaytan et al[6] using non-optimized melting process parameters.

In addition to the above mentioned build defects, non-uniformly distributed spherical voids (pores) of 1~6 μm in diameter are observed in all micrographs (Fig.3b). These pores are caused by argon (Ar) gas trapped in the gas atomized Ti-6Al-4V powder and can be removed by standard hot isostatic pressing (HIP) process for Ti alloys[6].

2.2 Microstructures

In general, the microstructures of EBM fabricated Ti-6Al-4V consist of columnar grains of prior β phase growing along the build direction across multiple build layers and Widmanstätten α platelets[12]. These microstructures are observed in all samples irrespective of different process parameter settings or thicknesses of test slab. The size, shape regularity and number of prior β columnar grains are different in samples built with different parameter settings and thicknesses. The summary of the microstructure observations is presented in Table 3.

The microstructures inside the prior β columnar grains are typical (α+β) Ti alloy, i.e., the Widmanstätten α platelets of different sizes and orientations, and the grain boundary α layer (α GB) along the grain boundary of prior β grain is observed. The length of α platelets depends upon the diameter of prior β columnar grain. In general, the α plate colony size is very small and not uniform, while in majority cases, α platelets are presented in singular form.

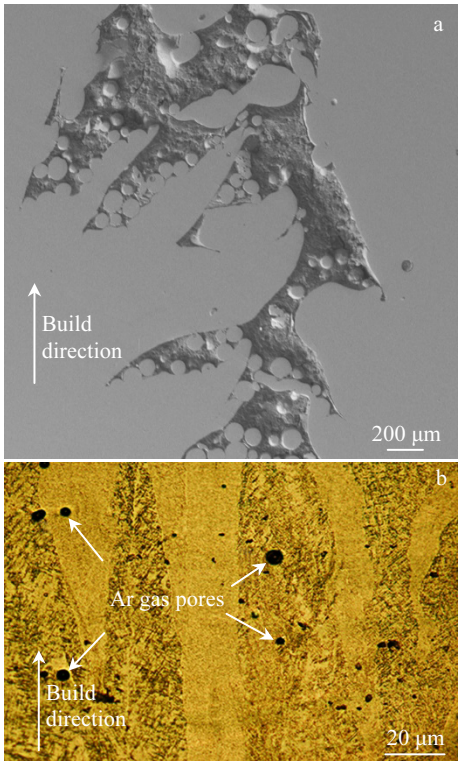

Fig.3 Microstructures of build defects: (a) undesired porosity and unmelted powder particles in sample built with offset focus of 30 mA; (b) non-uniform porosity due to trapped Ar gas

Table 3 Summary of microstructure observations

Sample code	Parameter value	Grain diameter/μm	Grain boundary α thickness/μm	Widmanstätten α platelet/μm		Rod-like β phase diameter/μm
				Width	Length	
S1Y1	δ=3.5 mm	3~5	1	1~2	8~25	0.2
S1Y2	δ=5.5 mm	10~40	1~3	1~3	5~60	0.2
S1Y3	δ=7.5 mm	20~70	1~3	1~4	5~60	0.2
C1X2	I=4 mA	2~13	-	1~2	60	0.2
C2X1	I=6 mA	2~13	-	1~2	60	0.2
S1X3	v=575 mm/s	5~50	1~3	1~4	40	0.2
S2X3	v=650 mm/s	6~35	1~3	1~4	20	0.2
S1X3	I_f=15 mA	5~50	1~3	1~4	3~25	0.2
S3X3	I_f=30 mA	6~35	1~3	1~4	3~15	0.2
SSL	l=10 mm	2~5	4	4	30	0.2
LSL	l=50 mm	2~10	5	2	20	0.2

Note: δ-thickness; I-current; v-scan speed; I_f-offset focus; l-scanning length; SSL-short scanning length; LSL-long scanning length

The β phase formed in the transformed prior β grain in the EBM produced Ti-6Al-4V was characterized by transmission electron microscopy (TEM)[12]. In EBM produced Ti-6Al-4V, β phase appears as rod-like structure on the grain boundary of the α platelets and generally grows along the build direction. The diameter of β phase rods is ~0.2 μm and is almost the same with that of other samples. The distance between two β phase rods is 0.5~2 μm.

The observed microstructure difference can be attributed to different factors affecting the microstructure development, i.e., the geometrical effects, power density of the beam and scanning strategy.

2.3 Geometrical effects

Through the microstructures of S-I samples built with different thicknesses and from different positions across the build, geometrical effect was studied. It is observed that with increasing the thickness of the test slab, the number and diameter of prior β columnar grain increase, the grains get a more regular shape and have regular orientation along the build direction, and microstructures become coarser (Fig.4a~4c).

In some cases, especially at bottom part of sample, grains are close to each other so they look like a bunch growing parallel to build direction. The columnar grains in the center part of the slab seem more regular in growing direction, i.e., more or less parallel to the build direction. While in the case of columnar grains near the surface and the thinnest sample, the growth direction often deviates from the build direction. Similar trends are observed when comparing the microstructure of two surfaces of sample: the wider surface (S-II) has characteristics of thicker sample in comparison to narrow surface (Fig.4c and 5a). In thick samples (Fig.5a and 5b), the grain boundary α phase (α GB) is quite smooth and regular and α platelets are fairly regular, although the α platelets are longer and coarser in thicker samples. The α platelets exhibit uneven and wavy morphology in thinner samples (Fig.4a).

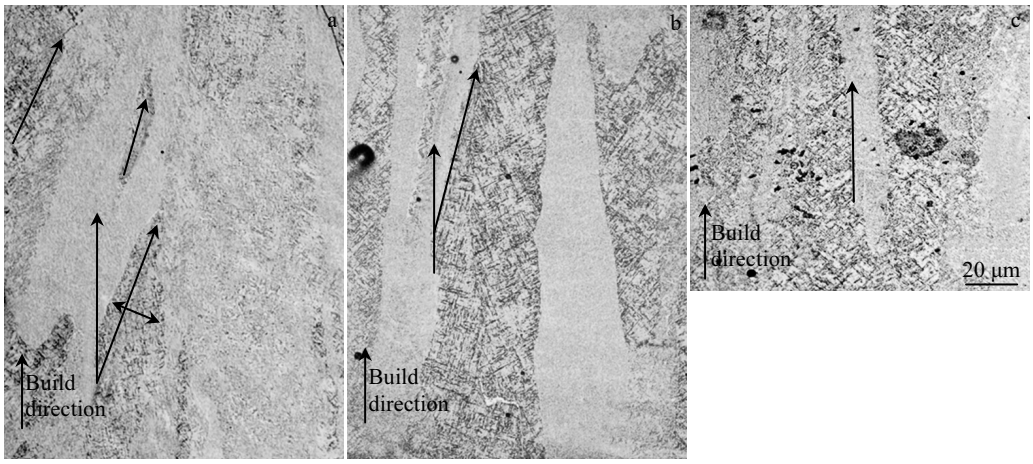

Fig.4 OM images of general microstructures of S-I samples built with scan speed of 575 mm/s, current of 9 mA, offset focus of 15 mA and thickness of 3.5 mm (a), 5.5 mm (b), and 7.5 mm (c) (single arrows indicate the growing direction angle of columnar grain in all micrographs)

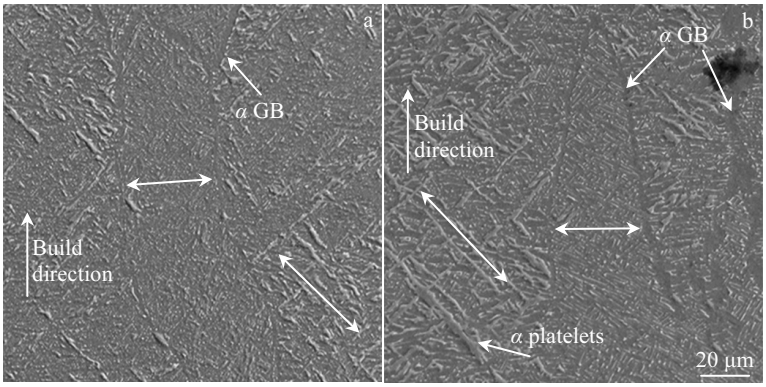

Fig.5 SEM images of general microstructure in the top part of S-I samples built with scan speed of 575 mm/s, beam current of 9 mA, offset focus of 15 mA and thickness of 5.5 mm (a) and 7.5 mm (b) (double sided arrows indicate the width of columnar grain or length of *α* platelets in all micrographs)

To study the effect of the height along the build direction on the microstructure, bottom part of sample is taken from the area less than 5 mm above the start plate, while the top part is taken from the area of slab at about 10 mm of the top of test slab. It is observed that the diameter of prior *β* columnar grain decreases with the increase of height of test slab, and the bunch of columnar grains is quite big in bottom part (Fig.6a and 6b).

2.4 Energy density of the beam

The energy density of the beam is the function of beam current, scan speed and offset focus. The energy density of the beam increases with increase of beam current and decreases with increase of scan speed and offset focus. Comparative study of microstructures was done for individual parameter of current, scan speed and offset focus.

In general, it is observed that with the increase of energy density, the number of columnar grains increases (Fig.7a and 7b). The grain boundary *α* layer is smoother in sample with higher energy density (Fig.4b), but in case of low energy density, the grain boundary *α* layer is wavy (Fig.7b). The bunch size of the columnar grain is higher for sample with higher energy density (Fig.6a and 7a). It is also observed that with decrease in energy density, the columnar grains are tilted (about 20°) in scanning direction, while in the case of high energy density, they follow the build direction (Fig.5a and 7a).

2.5 Scanning length

Fig.8 is the OM images of two samples produced with different scanning lengths. It is evident that the scanning length has quite an effect on the size and geometry of prior *β* columnar grains. For the samples with short scanning length, the grains are long but not very thick and their diameter is 2~5 μm. While for the samples with long scanning length, the geometry of the grains is quite irregular. The diameter of prior *β* grains varies irregularly along the build direction, and in some cases, the variation is as large as 10 μm. The respective grain boundaries in both cases are quite smooth and regular.

SEM micrograph in Fig.9 illustrates that (*α*+*β*) microstructures exist in both samples. The thickness and length of *α* platelets increase with decrease in scan length, while the width of *α* GB is unaffected by scanning length. In the cases of short scanning length, relatively bigger *α* plate colony size is observed.

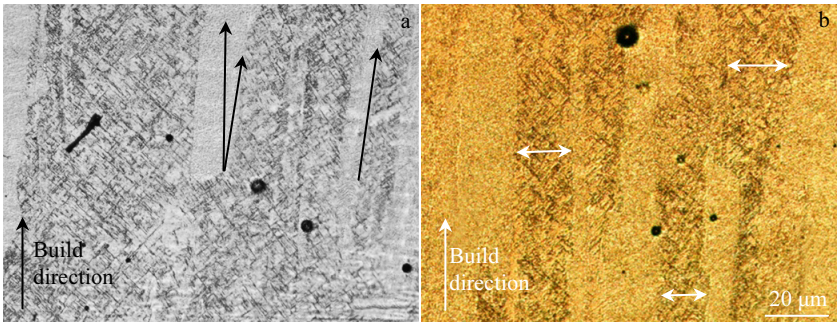

Fig.6 OM images of microstructures at the bottom (a) and top (b) part of S-II samples built with scan speed of 575 mm/s, beam current of 9 mA, offset focus of 15 mA and thickness of 7.5 mm

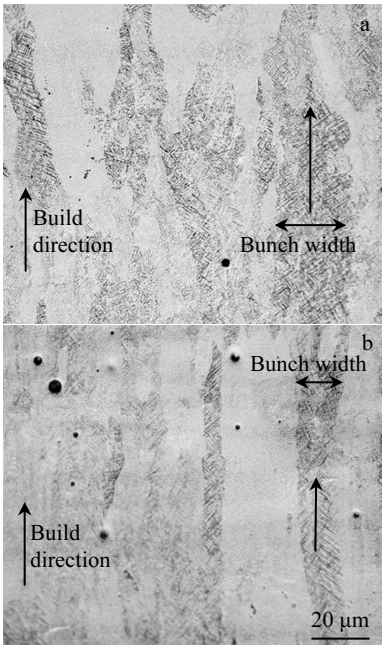

Fig.7 OM images of the bottom part of S-II samples built with scan speed of 250 mm/s, offset focus of 10 mA, slab thickness of 2.1 mm and beam current of 6 mA (a) and 4 mA (b)

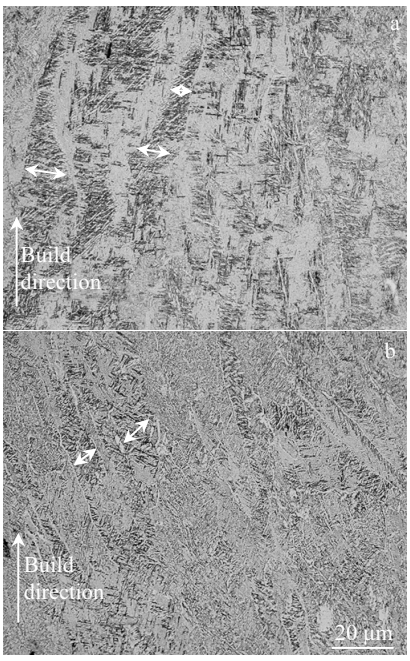

Fig.8 OM images of general microstructures of S-II samples built with scan length of 50 mm (a) and 10 mm (b)

3 Discussion

The microstructures of Ti-6Al-4V alloys depend on the heat

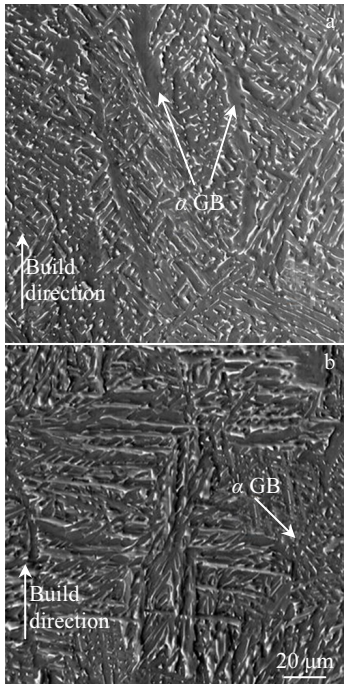

Fig.9 SEM images of general microstructures of S-II samples build with scan length of 50 mm (a) and 10 mm (b)

treatment and processing history[11]. For EBM built Ti-6Al-4V, the phase transformation from liquefied temperature (~1900 C) to room temperature after the build is a three-step procedure, i.e., rapid cooling from 1900 °C to 700 °C, isothermal hold at 700 °C for entire duration of build and slow cooling from 700 °C to room temperature.

The microstructures observed in all the cases are similar and dominated by columnar grains of prior β phase. Inside the prior β grains, the (α+β) structure consists of Widmanstätten α platelets and rod-like β phase formed on the grain boundaries of α platelets. The thickness and process parameter setting have a strong effect on the shape and size of columnar grain. With increasing the thickness of the sample, the diameter and height of the grains increase and also more regular geometry grains grow in parallel with the build direction. Considering the effects of process parameter settings, the height and diameter of the prior β grain increase with increase in energy density which is a function of scan speed, beam current and offset focus.

As reported by Al-Bermani[1] and Thijs[13] et al, the heat conduction direction during the solidification determines the orientation of the prior β grain in EBM. The formation of columnar grain occurs during the initial rapid cooling. The regular geometry of columnar grain depends upon the cooling rate, cooling path and melt pool size. For different parameter settings and thicknesses of the sample, the difference in grain diameter and geometry can be attributed to the difference in heat transfer in each case. In the case of thinner samples, due

to immediate contact with the surrounding powder, the columnar grains tend to tilt towards the outer sides of the build and deviation from build direction is observed. In thicker samples, tilting grain near the surface exists also due to the heat flow. In the case of thicker samples, due to the relatively big size of build, the heat flow can only transfer towards the base plate, especially in the central part of the build, hence more straight columnar grains are observed. Due to the multiple remelting during addition of every new thin layer, the columnar grains with smoother shape and coarser microstructure are observed. Similarly, in the case of builds with higher energy density, the builds exhibit larger and coarser columnar grains.

In the case of studying the effect of scanning length, although the samples are thicker than the samples used for other process parameter setting study, the columnar grains observed in these samples are much thinner. Also, in these samples, no bunching phenomenon is observed which is usually observed in thicker samples. The scanning lengths, in the case of other builds, cover across the whole melt plate which is about 150 mm. If we consider all the samples, it is observed that with increasing the scan length, the columnar grains become thicker and coarser. The reason for the observed difference is due to the fact that at turning point, the scan speed of the beam increases and thereby energy density of the beam decreases. For shorter scan length, this turning point area with low energy density beam contributes significantly in total area of the build surface, and hence smaller and thinner columnar grains are observed. In the case of long scanning length, turning points are far away and almost all the build is built with relatively high beam energy density, and hence thicker columnar grains and bunches are observed. Another possible reason for this difference is the time delay of the arrivals of successive beams. With short scanning length, the time difference between two successive arrivals of the beam at certain point is very small and the melt pool has shorter time to solidify. While in case of long scanning length, the time interval is longer. The long time delay between two successive remelting provides an opportunity for previous layer to get stable, resulting in coarser microstructure.

The formation of the grain boundary α and Widmanstätten α platelets starts when the temperature drops below the β transus temperature which is about 995±20 °C, and it mainly occurs during the isothermal hold at about 700 °C. At first, the grain boundary α phase (α GB) nucleates heterogeneously on the prior β columnar grains, and grows in directions normal to the grain boundaries to form an α layer. The α GB does not possess a certain orientation relationship with the prior β phase. After the formation of α GB, the Widmanstätten plates start to nucleate along the α GB allotriomorphs inside the prior β columnar grains[12,14]. It is speculated that the martensitic phase can form when the alloy Ti-6Al-4V is rapidly cooled down from 1900 °C to 700 °C [1]. If martensitic α' phase forms during the initial rapid cooling, the α' phase will be unstable in the build due to long hold duration at 700 °C. During the isothermal hold at about 700 °C, tempering of the martensitic phase occurs, and (α+β) structure can form. According to Mur et al[15], the transformation from martensite α' to (α+β) phase at isothermal hold of 700 °C in Ti-6Al-4V alloy is completed in ~30 min. The cooling rate for all the samples is identical and the test slabs are kept at 700 °C for more than 30 min, so the final microstructures in the EBM produced parts should be (α+β) structure. The difference in length of α platelets is due to the different size of prior β columnar grains. The α platelets nucleate at grain boundary and grow up until they meet other α colonies or platelets originated from other nucleation sites. Hence the maximum possible length of platelet is less than the length of prior β grain, and α platelets with different lengths are observed.

The β phase rods also form during the formation of (α+β) structure at isothermal hold when the temperature falls below the β transus temperature. Since the cooling rate and isothermal hold are similar for all samples in every build, no difference in diameter of the β phase rods is observed in all the samples irrespective of the sample thickness or process parameter setting.

4 Conclusions

1) Microstructures of Ti-6Al-4V consist of columnar grains of prior β phase growing along the build direction.

2) The height and diameter of prior β columnar grain is affected by the sample thickness and process parameters. The height and diameter of the prior β columnar grain increase with the increase of sample thickness and energy density of the beam. The diameter of prior β columnar grains increases with increase in scanning length.

3) The β phase of rod-like structure forms at grain boundaries of the α grain, with growing direction parallel to build direction in majority cases.

References

1 Al-Bermani S S, Blackmore M L, Zhang W *et al*. *Metallurgical and Materials Transactions A*[J], 2010, 41(13): 3422

2 Cormier D, Harrysson O, West H. *Rapid Prototyping Journal*[J], 2004, 10(1): 35

3 Galati M, Iuliano L. *Additive Manufacturing*[J], 2018, 19: 1

4 Pobel C R, Osmanlic F, Lodes M A *et al*. *Rapid Prototyping Journal*[J], 2019, 25(4): 665

5 Murr L E, Esquivel E V, Quinones S A *et al*. *Materials Characterization*[J], 2009, 60(2): 96

6 Gaytan S M, Murr L E, Medina F *et al*. *Materials Technology*[J], 2013, 24(3): 180

7 Parthasarathy J, Starly B, Raman S *et al*. *Journal of the Mechanical Behavior of Biomedical Materials*[J], 2010, 3(3): 249

8 Zhang L C, Liu Y J, Li S J *et al*. *Advanced Engineering*

Materials[J], 2018, 20(5): 1 700 842
9 Zeng L, Bieler T R. *Materials Science and Engineering A*[J], 2005, 392(1-2): 403
10 Sokolov Y A, Afanas'Eva L E, Barabonova I A *et al*. *Metal Science and Heat Treatment*[J], 2015, 57(5-6): 354
11 Lütjering G. *Materials Science and Engineering A*[J], 1998, 243(1-2): 32
12 Safdar A, Wei L Y, Snis A *et al*. *Materials Characterization*[J], 2012, 65: 8
13 Thijs L, Verhaeghe F, Craeghs T *et al*. *Acta Materialia*[J], 2010, 58(9): 3303
14 Appolaire B, Héricher L, Aeby-Gautier E. *Acta Materialia*[J], 2005, 53(10): 3001
15 Mur F X G, Rodriguez D, Planell J A. *Journal of Alloys and Compounds*[J], 1996, 234(2): 287

工艺参数设置和厚度对电子束熔融加工 Ti-6Al-4V 合金微观结构的影响

贺怀志[1,2,3]，Safdar Adnan[1]，魏鎏英[1]
(1. 马尔默大学 材料科学学院，瑞典 马尔默 SE-205 06)
(2. 哈尔滨工业大学 先进焊接与连接国家重点实验室，黑龙江 哈尔滨 150001)
(3. 哈尔滨电气集团有限公司 中央研究院，黑龙江 哈尔滨 150028)

摘　要：研究了试件尺寸和工艺参数（电子束强度，扫描速度，焦点偏移量和扫描长度）对电子束熔融（EBM）加工 Ti-6Al-4V 合金微观结构的影响。结果表明，可以观察到 EBM 加工的 Ti-6Al-4V 合金的微观结构由原始 β 相的柱状晶粒组成。在柱状晶粒内部观察到典型的（α+β）结构，即魏氏体 α 片和在细小的 α 晶粒的界面上形成的杆状 β 相。还发现沿原始 β 柱状晶粒的晶界形成的 α 层晶界。随着试件厚度、电子束能量密度和扫描长度的增加，先前的 β 柱状晶粒的直径增大，并且生长的方向与加工方向一致。同时，柱状晶粒直径随着试件高度的增加而减小。随着试件厚度和电子束能量密度的增加，α 片会变得更粗大。

关键词：Ti-6Al-4V；电子束熔融；工艺参数

作者简介：贺怀志，男，1984 年生，硕士，哈尔滨电气集团有限公司中央研究院，黑龙江 哈尔滨 150028，电话：0451-58590367，E-mail: hehz@harbin-electric.com